Inorganic Chemistry

Article

pubs.acs.org/IC

Structural and Vibrational Properties of $U(VI)O_2Cl_4^{2-}$ and $Pu(VI)O_2Cl_4^{2-}$ Complexes

David D. Schnaars and Richard E. Wilson*

Chemical Sciences and Engineering Division, Argonne National Laboratory, 9700 S. Cass Avenue, Argonne, Illinois 60439, United States

Supporting Information

ABSTRACT: In actinide chemistry, it has been shown that equatorial ligands bound to the metal centers of actinyl ions have a strong influence on the chemistry and therefore the electronic structure of the O═An═O moiety. While this influence has received a significant amount of attention, considerably less research has been done to investigate how the identity of the actinide metal itself (U, Np, Pu, Am) affects the actinyl stretching frequencies. Herein, we present the structural and spectroscopic characterization of six actinyl tetrachloride compounds ($M_2AnO_2Cl_4$: M = Rb, Cs, Me_4N; An = U, Pu) as well as the stretching and interactive force constants of the actinyl moiety in each species. Our results show a decrease in the stretching force constant and a weakening of the An═O bond when traversing the actinides from uranyl to plutonyl, which is interesting because the solid state molecular structures show a slight contraction of the An═O bond length when uranium is replaced with plutonium. Additionally, the interaction force constants for both the uranyl and plutonyl compounds were found to be negative, which corresponds to a reduction of the force constant for the symmetric stretching mode.

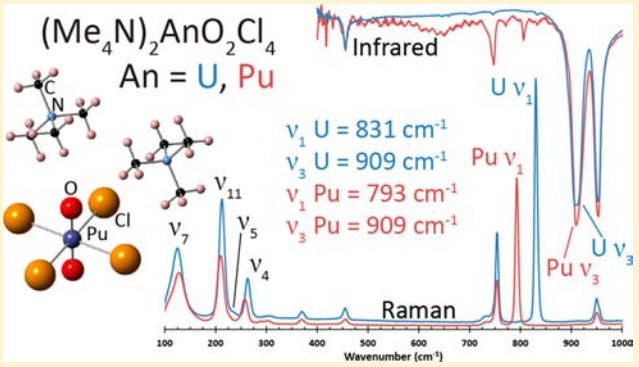

INTRODUCTION

The actinyl moiety, O═An═O, is composed of two oxygen ligands tightly bound to an actinide atom in a linear conformation and is the most common configuration of high valent early actinides in aqueous conditions. These -yl actinide−oxygen bonds are known to be short, strong, and typically unreactive. The strength of the actinyl bond can be seen in the bond dissociation constant for the U═O bond in uranyl, 604 kJ/mol,[1] which is 72 kJ/mol higher than the C═O bond in CO_2 (532 kJ/mol).[2] Unlike the bent O═TM═O arrangement typically found in transition metal dioxo compounds such as $MoO_2(Ph_3PO)_2Cl_2$,[3,4] the linear conformation of the actinyl moiety arises from participation of the actinide f-orbitals in bonding, which is not possible in the analogous transition metal−ligand bonds. The primary coordination sphere of the actinide center is completed with 3−6 co-ligands that are typically restricted to the equatorial plane of the actinyl moiety.[5] While these equatorial ligands are known to be weakly bound and relatively labile in comparison to the actinyl oxos, it has been shown that they have a strong influence on the chemistry and therefore the electronic structure of the actinyl moiety.

The influence of the equatorial ligands upon the actinyl moiety can be seen when comparing the oxo ligand exchange rates for $UO_2(H_2O)_5^{2+}$ and $UO_2(OH)_5^{3-}$. Under acidic conditions, the half-life for oxo ligand exchange in $UO_2(H_2O)_5^{2+}$ has been determined to be ∼40 000 h,[6,7] with faster rates typically requiring a photoexcitation of the uranyl ion.[8−10] Interestingly, placing the uranyl moiety in an alkaline environment and therefore replacing the equatorial water molecules with hydroxide ligands results in a dramatic increase of the oxo ligand exchange rate to a half-life of less than one second at room temperature.[6] Additionally, influence of the equatorial ligands upon the electronic structure of the actinyl moiety can be indirectly probed through shifts in the symmetric and asymmetric stretching frequencies observed using Raman and infrared spectroscopy, respectively. For example, Raman spectra of $UO_2(H_2O)_5^{2+}$ show the symmetric stretching frequency of the actinyl moiety located at 869 cm^{-1}.[11] Replacing the water ligands with hydroxide to form $UO_2(OH)_5^{3-}$ results in a shift of the symmetric stretching frequency to 786 cm^{-1}, indicating a perturbation to the electronic structure of the uranyl.[6]

Currently, there are two theories used to explain why the equatorial ligands influence vibrational properties of the actinyl moiety. The first theory is that upon complexation, the equatorial ligands compete with the -yl oxo ligands for the 6d orbitals of the actinide metal, resulting in changes to the actinyl bonding framework.[6,12−14] The second theory says that the changes in the electronic structure of the actinyl moiety are principally electrostatic in nature and influenced by the donor−

Received: August 1, 2013
Published: November 20, 2013

   dx.doi.org/10.1021/ic401991n | Inorg. Chem. 2013, 52, 14138−14147

acceptor ability of the equatorial ligands.[12,13,15−17] The latter idea was recently supported in a theoretical study by Vallet et al. where they used a point-charge model to determine that pure electrostatic interactions play a significant role in the uranyl bond destabilization for $[UO_2Cl_4]^{2-}$ in comparison to $[UO_2(H_2O)_5]^{2+}$.[18] While the origin of this phenomenon may be under debate, numerous studies have established correlations between the equatorial ligands and the actinyl vibrational frequencies.[13,17,19−22] These correlations have been used as guides to assist in the activation and functionalization of the uranyl oxo ligands,[23,24] which has become an area of interest for actinide organometallic chemistry over the past few years.[13,25−30]

While the influence of equatorial ligands on the electronic structure of the actinyl moiety has received a significant amount of attention, considerably less research has been done to investigate how the identity of the actinide metal itself (U, Np, Pu, Am) affects the actinyl stretching frequencies. The complexes presented here provide a unique opportunity for the structural and spectroscopic comparison of uranyl and plutonyl analogues. Through this comparison, we are able to investigate influences of f-electrons at the metal center upon the electronic structure of the actinyl moiety.

In this Article, we have two primary objectives. Our first objective is to compare how the vibrational frequencies of the actinyl moiety are affected as a function of the actinide metal center, i.e., the number of f-electrons, when going across the actinide series from uranium to plutonium. Using a valence bond potential model, we are able to quantify this difference in the vibrational spectra of uranium and plutonium by calculating the stretching force constants (k_1) and interaction force constants (k_{12}) for the isostructural uranyl and plutonyl compounds. By comparing isostructural uranyl and plutonyl compounds, we hope to be able to attribute changes in the vibrational spectra of the actinyl moiety to differences in the metal centers, specifically the number of f-electrons present where Pu(VI) has two f-electrons and U(VI) has none.

Our second objective is to investigate the influence of the secondary coordination sphere upon the electronic structure of the actinyl moiety and determine whether or not we can detect these more distant interactions using Raman and infrared spectroscopy. This is done through analysis of uranyl and plutonyl tetrachloride compounds with varying cations to try and measure the influence of the cation−anion interaction on the electronic structure of the actinyl moiety. Herein, we present the structural and spectroscopic characterization of six actinyl tetrachloride compounds ($M_2AnO_2Cl_4$: M = Rb, Cs, Me_4N; An = U, Pu) as well as the stretching and interactive force constants for each species.

EXPERIMENTAL SECTION

Caution! *Depleted uranium and ^{242}Pu are alpha-emitting isotopes. All experiments described were performed in specially designed laboratories with negative pressure fume hoods and gloveboxes, using strict radiological controls.*

The following reactions were performed under ambient conditions, and all materials, with the exception of depleted uranium and ^{242}Pu, were obtained from commercial sources and used as received unless otherwise noted. A stock solution of ^{242}Pu was prepared using standard ion-exchange techniques where a ^{242}Pu(IV) solution in 7.5 M HNO_3 was loaded onto a DOWEX anion exchange column conditioned in the nitrate form. The column was then washed with several volumes of 7.5 M HNO_3 to remove cationic and anionic impurities. The plutonium was eluted from the column using 1 M HCl and subsequently heated with periodic additions of 11 M HCl to drive off residual nitric acid and reduce its volume resulting in a solution of primarily Pu(IV) and Pu(VI). The solution was then oxidized to the hexavalent state by bubbling with ozone for three days. Oxidation state purity of the Pu was determined by optical spectrometry.

Vibrational Spectroscopy. Infrared samples were diluted (∼1−5 wt %) with dry KBr and pressed into a pellet before being collected on a Nicolet Nexus 870 FTIR system. Data were collected using 16 scans over 4000−400 cm^{-1} with a resolution of 2 cm^{-1}. Raman data were collected on randomly oriented single crystals using a Renishaw inVia Raman microscope with a circularly polarized excitation line of 532 or 785 nm.

X-ray Crystallography. The solid state molecular structures for the complexes presented here were determined similarly with exceptions noted. Crystals were mounted on a glass fiber under Paratone-N oil. Full spheres of data (0.5° frame widths) were collected using a Bruker SMART or QUAZAR diffractometer equipped with an APEXII detector using Mo Kα radiation. Frame exposures of 15 s were used for compounds **U-Rb**, **U-Cs**, and **Pu-Rb**, while 20 s exposures were used for compounds **U-Me$_4$N**, **Pu-Cs**, and **Pu-Me$_4$N**. All data were collected at 100 K using an Oxford Cryosystems cryostat. The data were integrated and corrected for absorption using the APEX2 suite of crystallographic software, while structure solutions and refinements were completed using XShell.[31]

For compounds **U-Me$_4$N** and **Pu-Me$_4$N**, solvent accessible voids of 42 and 41 Å^3, respectively, were observed within the crystal lattice. The difference Fourier maps for **U-Me$_4$N** reveal residual electron density located ∼3.22 Å from the nearest chloride ligand and 3.39 Å from the nearest methyl carbon. Similarly, the difference Fourier maps in **Pu-Me$_4$N** show residual electron density located ∼3.26 and ∼3.36 Å from the nearest chloride ligand and methyl carbon, respectively. In both compounds, these distances are consistent with water behaving as a hydrogen bond donor to the chloride ligand[32] and a hydrogen bond acceptor from the Me_4N^+ cation.[33] While this evidence suggests the presence of water molecules within the crystal lattice, we were unable to confidently refine a water molecule due to a low partial occupancy. Upon assignment of the residual electron density as oxygen, refinement results in partial occupancy for the oxygen of 16% in **U-Me$_4$N** and 22% in **Pu-Me$_4$N**. Additionally, application of the SQUEEZE[34] technique to these compounds determined 4 or 5 electrons are present within each of the voids, which is consistent with a 20−25% occupancy for two water molecules, where the second water is generated by symmetry.

Synthesis for Compounds U-Rb, U-Cs, and U-Me$_4$N. In a 2 mL shell vial, 20 mg (0.070 mmol) of UO_3 was dissolved using 200 μL of 2.0 M HCl forming a yellow solution. To this solution was added 70 μL of 2.0 M MCl (M = Rb, **U-Rb**; Cs, **U-Cs**; Me_4N, **U-Me$_4$N**) (0.14 mmol) and 200 μL of H_2O resulting in a less intense yellow solution. The solution was allowed to evaporate at room temperature for several days resulting in the deposition of crystalline material. $Rb_2UO_2Cl_4 \cdot 2H_2O$ (**U-Rb**) was isolated as yellow plates in quantitative yield after complete evaporation of the solution, while $Cs_2UO_2Cl_4$ (**U-Cs**) was isolated as yellow-green rods (37.1 mg, 78% yield) and $[Me_4N]_2UO_2Cl_4$ (**U-Me$_4$N**) was isolated as yellow-green blocks (33.7 mg, 86% yield). A list of peak information and assignments for the Raman and infrared spectra of **U-Rb**, **U-Cs**, and **U-Me$_4$N** is located in the Supporting Information.

Synthesis for Compounds Pu-Rb, Pu-Cs, and Pu-Me$_4$N. A 2 mL shell vial was charged with 200 μL of 0.062 M ^{242}Pu (3 mg, 0.012 mmol) dissolved in concentrated HCl. To this orange solution was added 250 μL of 0.11 M MCl (M = Rb, **Pu-Rb**; Cs, **Pu-Cs**; Me_4N, **Pu-Me$_4$N**) (0.022 mmol) in concentrated HCl, resulting in a less intense orange solution. Evaporation of the solution within a fume hood (several weeks) resulted in the deposition of the desired product ($Rb_2PuO_2Cl_4$, **Pu-Rb**; $Cs_2PuO_2Cl_4$, **Pu-Cs**; $[Me_4N]_2PuO_2Cl_4$, **Pu-Me$_4$N**) as irregular orange crystals. The small scale of these reactions precludes the ascertainment of an accurate yield. A list of peak information and assignments for the Raman and infrared spectra of **Pu-Rb**, **Pu-Cs**, and **Pu-Me$_4$N** is located in the Supporting Information.

dx.doi.org/10.1021/ic401991n | *Inorg. Chem.* 2013, 52, 14138−14147

Table 1. X-ray Crystallographic Data for Complexes U-Rb, U-Cs, U-Me_4N, Pu-Rb, Pu-Cs, and Pu-Me_4N

	U-Rb	U-Cs	U-Me_4N	Pu-Rb	Pu-Cs	Pu-Me_4N
empirical formula	$Cl_4H_4O_4Rb_2U$	$Cl_4Cs_2O_2U$	$Cl_4H_{24}C_8O_2N_2U$	$Cl_4O_2PuRb_2$	$Cl_4O_2PuCs_2$	$Cl_4H_{24}C_8O_2N_2Pu$
cryst habit, color	plate, yellow-green	plate, yellow-green	prismatic, yellow-green	irregular, orange	prismatic, orange	irregular, orange
cryst size (mm^3)	0.22 × 0.15 × 0.05	0.54 × 0.10 × 0.04	0.19 × 0.11 × 0.10	0.63 × 0.29 × 0.24	0.39 × 0.17 × 0.10	0.17 × 0.15 × 0.12
cryst syst	triclinic	monoclinic	tetragonal	monoclinic	monoclinic	tetragonal
space group	$P\bar{1}$	$C2/m$	$P4_2/mnm$	$C2/m$	$C2/m$	$P4_2/mnm$
V (Å^3)	292.90(5)	514.4(3)	948.72(18)	470.1(2)	514.52(15)	944.3(2)
a (Å)	6.7500(7)	11.829(5)	9.1341(10)	11.383(3)	11.785(2)	9.0962(13)
b (Å)	6.8991(7)	7.648(3)	9.1341(10)	7.534(2)	7.6934(13)	9.0962(13)
c (Å)	7.4230(7)	5.781(2)	11.3712(12)	5.5028(14)	5.7285(10)	11.4129(17)
α (deg)	92.1910(10)	90	90	90	90	90
β (deg)	101.6700(10)	100.385(4)	90	94.959(3)	97.856(2)	90
γ (deg)	118.8110(10)	90	90	90	90	90
Z	1	2	2	2	2	2
fw (g/mol)	618.80	677.65	560.12	586.74	681.62	564.09
density (calcd) (Mg/m^3)	3.508	4.375	1.961	4.145	4.400	1.984
abs coeff (mm^{-1})	22.993	23.731	9.112	18.368	14.358	4.050
F_{000}	270	572	524	504	576	528
total no. reflns	4828	3415	15 574	3844	3133	13 515
unique reflns	2005	765	1042	904	636	834
final R indices [$I > 2\sigma(I)$]	R1 = 0.0194	R1 = 0.0340	R1 = 0.0207	R1 = 0.0291	R1 = 0.0189	R1 = 0.0227
	wR2 = 0.0441	wR2 = 0.0963	wR2 = 0.0481	wR2 = 0.0758	wR2 = 0.0488	wR2 = 0.0581
largest diff. peak and hole (e^- Å^{-3})	1.430 and −2.000	4.234 and −3.479	2.040 and −0.525	5.610 and −3.434	0.753 and −2.312	2.158 and −0.703
GOF	1.143	1.079	1.126	1.171	1.323	1.131

RESULTS

Structural Descriptions. The solid state molecular structures for complexes **U-Rb**,[35] **U-Cs**,[36,37] **U-Me_4N**,[38] and **Pu-Cs**[39] have been previously reported. Here, we briefly present the crystallographic details and arrangement of the anion again for the purposes of discussion. We also expand upon literature reports through our discussion of the cation−anion interactions, since the only two compounds for which they were previously mentioned are **U-Rb**[35] and **U-Cs**,[36] the latter of which was later shown to have significant errors.[37] Additionally, to standardize the varying collection temperatures of the previously reported structures, we have recollected the data at 100 K to ensure uniform conditions and allow for a more accurate structural comparison between complexes.

The six complexes discussed here crystallize in three crystal systems; triclinic (**U-Rb**: $P\bar{1}$), monoclinic (**U-Cs**, **Pu-Rb**, and **Pu-Cs**: $C2/m$), and tetragonal (**U-Me_4N** and **Pu-Me_4N**: $P4_2/mnm$) (Table 1). The composition of the anion is identical for each compound and consists of six ligands bound to the metal center in a pseudo-octahedral geometry. The axial positions are occupied by the two -yl oxo ligands, while the four chloride ligands reside in the equatorial plane (Figure 1). In each case, the actinyl anion is charge balanced by the presence of two monocations, the identity of which are varied in this study (Rb, Cs, Me_4N). All of the complexes presented herein crystallize in centrosymmetric space groups where the actinide atom resides on a special position with either C_i, C_{2h}, or D_{2h} site symmetry, resulting in a strictly linear conformation of the actinyl moiety in these complexes.

For the three uranium compounds presented herein (**U-Rb**, **U-Cs**, and **U-Me_4N**), the average bond distances for the U═O and U—Cl bonds are 1.77(1) and 2.67(1) Å, respectively (Table 2). These bond lengths are consistent with previously reported uranyl tetrachloride compounds such as

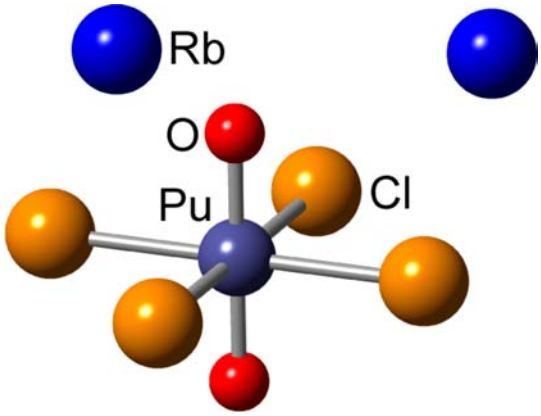

Figure 1. Ball and stick model of $Rb_2PuO_2Cl_4$ (**Pu-Rb**) depicting the connectivity around the metal center along with the charge balancing cations.

$[Et_4N]_2UO_2Cl_4$ (U═O, 1.76(2) and 1.77(3) Å; U—Cl, 2.65(1)−2.68(1) Å),[40] $[(NH_4)(5\text{-crown-}5)_2]_2UO_2Cl_4\cdot 2MeCN$ (U═O, 1.763(5) Å; U—Cl, 2.645(2) and 2.682(2) Å),[41] and $[SN_2C_{10}H_9]_2UO_2Cl_4$ (U═O, 1.77(1) Å; U—Cl, 2.662(5) and 2.665(5) Å).[42] Upon moving across the actinide series to plutonium (compounds **Pu-Rb**, **Pu-Cs**, and **Pu-Me_4N**), the average metal An═O bond length decreases 0.02 Å to 1.75(1) Å, while the An—Cl bond contracts 0.01 Å to 2.66(1) Å (Table 2). This shortening of the actinide−ligand bond lengths is consistent with the decrease in ionic radii when going across the series from uranium (6 coordinate U^{VI}: 0.73 Å) to plutonium (6 coordinate Pu^{VI}: 0.71 Å).[43] As with the uranium compounds, the bond lengths of the plutonium compounds are consistent with previously reported plutonyl chloride compounds such as $[Ph_3PNH_2]_2[PuO_2Cl_4]$ (Pu═O, 1.709(10) and 1.718(9) Å; Pu—Cl, 2.641(4)−2.661(4) Å),[44]

dx.doi.org/10.1021/ic401991n | Inorg. Chem. 2013, 52, 14138−14147

Table 2. Selected Bond Lengths for Complexes U-Rb, U-Cs, U-Me_4N, Pu-Rb, Pu-Cs, and Pu-Me_4N

compound	An=O (Å)	An—Cl (Å)
Uranium		
$Rb_2UO_2Cl_4{\cdot}2H_2O$ (**U-Rb**)	1.773(2)	2.665(1)
		2.669(1)
$Cs_2UO_2Cl_4$ (**U-Cs**)	1.776(6)	2.670(1)
$[Me_4N]_2UO_2Cl_4$ (**U-Me_4N**)	1.766(4)	2.648(1)
		2.677(1)
average[a]	1.77(1)	2.67(1)
Plutonium		
$Rb_2PuO_2Cl_4$ (**Pu-Rb**)	1.754(5)	2.663(1)
$Cs_2PuO_2Cl_4$ (**Pu-Cs**)	1.750(4)	2.663(1)
$[Me_4N]_2PuO_2Cl_4$ (**Pu-Me_4N**)	1.745(5)	2.634(2)
		2.660(2)
average[a]	1.75(1)	2.66(1)

[a]Error for average bond lengths is calculated as the standard deviation.[46]

Table 3. Shortest Cation···Anion and Solvent···Anion Interactions for Complexes U-Rb, U-Cs, U-Me_4N, Pu-Rb, Pu-Cs, and Pu-Me_4N[a]

compound	Cat···O_{yl} (Å)		Cat···Cl (Å)	
U-Rb	3.019(2)		3.335(1)	
U-Cs	3.275(6)		3.512(2)	
Pu-Rb	3.540(5)		3.315(1)	
Pu-Cs	3.495(4)		3.489(1)	
compound	H···O_{yl} (Å)	C—H···O_{yl} (deg)	H···Cl (Å)	C—H···Cl (deg)
U-Me_4N	2.65(4)	142(3)	2.94(4)	133(3)
Pu-Me_4N	2.62(6)	139(5)	2.94(5)	129(4), 167(5)

[a]Distances given for Rb and Cs interactions are from the center of the atom, while distances given for Me_4N interactions are from the closest H atom.

$PuO_2Cl_2(Ph_3PO)_2$ (Pu=O, 1.747(4) Å; Pu—Cl, 2.630(2) Å),[44] and $[PuO_2Cl_2(THF)_2]_2$ (Pu=O, 1.714(9) and 1.725(9) Å; Pu—$Cl_{terminal}$, 2.645(4) Å).[45]

Compounds **U-Rb** and **Pu-Rb** are charge balanced by Rb cations, while **U-Cs** and **Pu-Cs** contain Cs. For these compounds, the shortest cation···Cl and cation···O_{yl} separations are 3.335(1) and 3.019(2) Å (**U-Rb**), 3.512(2) and 3.275(6) Å (**U-Cs**), 3.315(1) and 3.540(5) Å (**Pu-Rb**), and 3.489(1) and 3.495(4) Å (**Pu-Cs**), respectively (Figure 2) (Table 3). In all four compounds the cation···Cl and cation···O_{yl} distances are equal to or slightly longer than the combined ionic radii of the participating atoms (Cl^-, 1.81 Å; Cs^+ (8 coordinate), 1.74 Å; O^{2-}, 1.35 Å; Rb^+ (8 coordinate), 1.61 Å; Rb^+ (7 coordinate), 1.56 Å),[43] but they are significantly shorter than the combined van der Waals radii (Cl, 1.75 Å; Cs, 3.43 Å; O, 1.52 Å; Rb, 3.03 Å).[47,48] We believe any anion—cation interaction should be weak due to the elongated interatomic distances and low charge—ionic radius ratio of the Rb and Cs atoms (for 8-coordinate cations: Rb^+, 0.62; Cs^+, 0.57; as a reference Li^+, 1.08).[43,49] In addition to the compounds presented here, similar cation···O_{yl} interactions have been observed in previously reported uranyl compounds with alkali metal cations.[23,50−53]

In the Rb and Cs compounds, the cation—Cl distances are very similar for both the uranyl and plutonyl analogue, while the cation—O distance increases when going across the actinides from uranium to plutonium. The longer cation—O interaction for the plutonium analogues may be caused by the less negative effective charge on the -yl oxygen atoms of plutonyl in comparison to uranyl,[54−56] which would result in a weaker cation—O interaction. This argument also supports the similar cation—Cl distances observed for the uranium and plutonium analogues because the effective charge of the chloride ligands would not vary significantly based on the identity of the actinide due to their primarily ionic interaction with the metal center.

In compounds **U-Me_4N** and **Pu-Me_4N**, the methyl groups on the Me_4N^+ cation weakly interact with the chloro and oxo ligands of the actinyl anion (Figure 2, Table 3). The shortest C—H···Cl interactions for the two compounds are 2.94(4) Å (**U-Me_4N**) and 2.94(5) Å (**Pu-Me_4N**), which is consistent with previously reported values for C—H···Cl_M (mean: 2.876 Å, where Cl_M signifies that the Cl is bound to a metal).[57] For interactions with the actinyl oxygen, the shortest C—H···O_{yl} separations (2.65(4) Å (**U-Me_4N**) and 2.62(6) Å (**Pu-Me_4N**)) are significantly longer than previously reported values for hydrogen bonding interactions to the -yl oxygen ligand (1.665(13)—2.39(3) Å),[58] indicating a very weak anion···cation interaction. The increased distance of these interactions is most likely due to the single positive charge spread over the entire Me_4N^+ cation and the low donor strength of the C—H moiety resulting from the inherently nonpolar nature of the methyl groups.[32]

In addition to the anion and cations, complex **U-Rb** contains an unbound water molecule within the crystal lattice. The hydrogen atoms of the water molecule are oriented toward the equatorial chloride ligands of the anion suggesting a potential hydrogen bonding interaction, but the $O_{solvent}$···Cl (3.317(3) Å) and $O_{solvent}$—H···Cl (2.69(5) Å) distances are significantly longer than the reported average hydrogen bonding interactions for H_2O (3.190(3) and 2.237(3) Å, respectively)[32] (Table 3). These elongated distances indicate that if a hydrogen

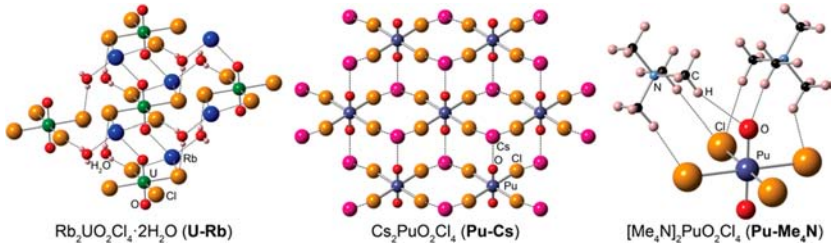

Figure 2. Ball and stick models showing a sample of the cation—anion interactions in $Rb_2PuO_2Cl_4{\cdot}2H_2O$ (**U-Rb**) (left), $Cs_2PuO_2Cl_4$ (**Pu-Cs**) (middle), and $[Me_4N]_2PuO_2Cl_4$ (**Pu-Me_4N**) (right). Dashed lines indicate cation—anion interactions. U = green, Pu = purple, O = Red, Cl = orange, Rb = dark blue, Cs = magenta, N = light blue, C = black, H = beige.

dx.doi.org/10.1021/ic401991n | Inorg. Chem. 2013, 52, 14138−14147

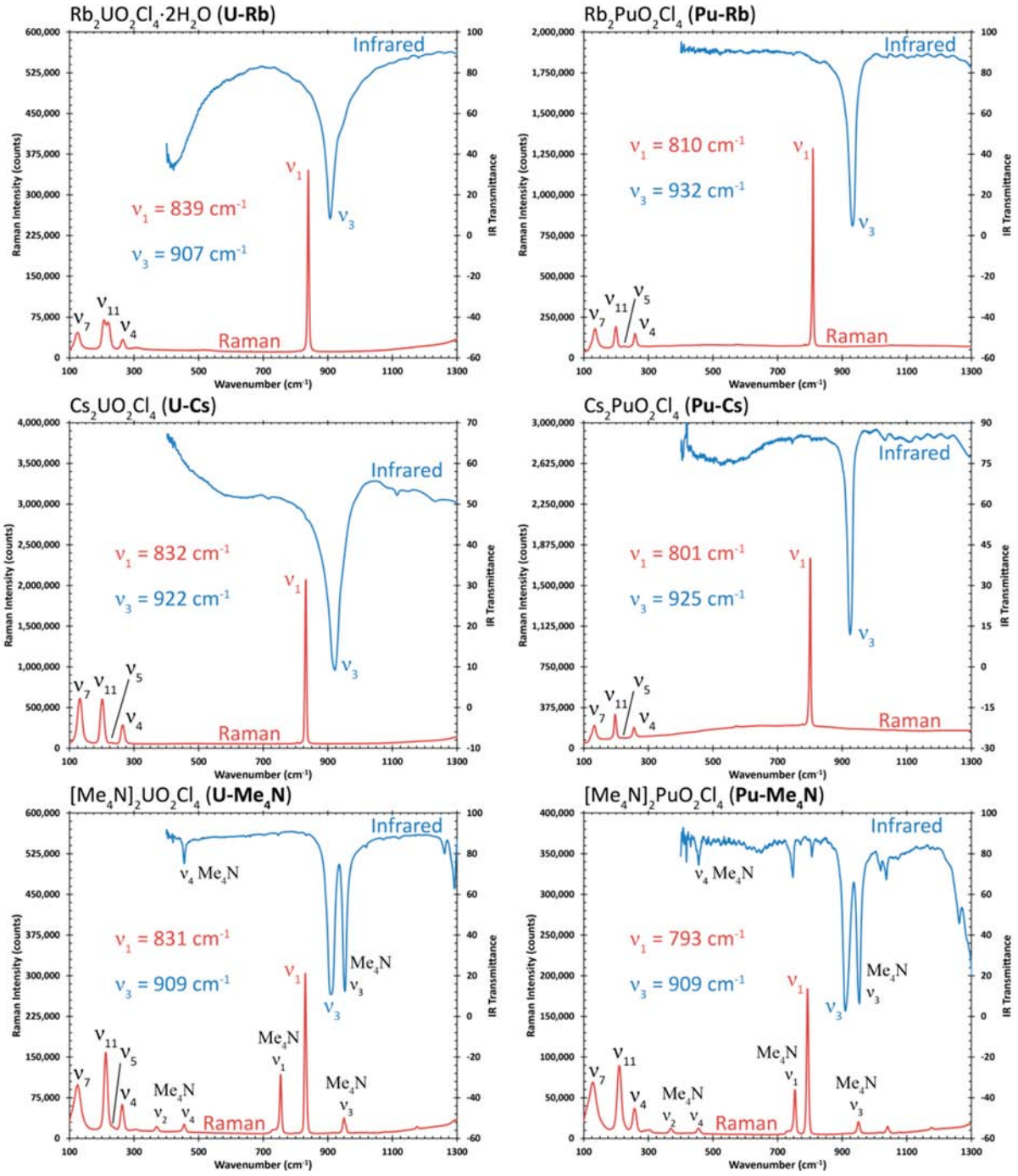

Figure 3. Infrared (blue) and Raman (red) spectra for $Rb_2UO_2Cl_4{\cdot}2H_2O$ (**U-Rb**) (upper left), $Cs_2UO_2Cl_4$ (**U-Cs**) (middle left), $[Me_4N]_2UO_2Cl_4$ (**U-Me$_4$N**) (lower left), $Rb_2PuO_2Cl_4$ (**Pu-Rb**) (upper right), $Cs_2PuO_2Cl_4$ (**Pu-Cs**) (middle right), and $[Me_4N]_2PuO_2Cl_4$ (**Pu-Me$_4$N**) (lower right).

bonding interaction is occurring between the lattice water and the chloride ligands of the anion, it is most likely very weak.

Vibrational Spectroscopy. In addition to single crystal X-ray diffractometry, the complexes presented herein have also been characterized using Raman and infrared spectroscopy. While the vibrational spectroscopy of **U-Rb**,[59−62] **U-Cs**,[61−71] **U-Me$_4$N**,[62,63,67,72,73] and **Pu-Cs** (photoluminescence)[74] has been previously investigated, to our knowledge this is the first instance where the Raman and infrared spectra of the plutonyl species have been collected and compared to their uranyl analogues. We have collected the Raman and infrared data for all six compounds to ensure similar conditions and allow for an accurate comparison between uranium and plutonium analogues.

The actinide complexes in these structures are ideally D_{4h} symmetry, and therefore, 15 vibrational modes may be expected to arise from the anion. For the $AnO_2Cl_4^{2-}$ anion, the vibrational frequencies associated with the equatorial ligand modes are much lower in frequency than the stretching modes of the actinyl moiety. As such, we should not expect any coupling between these vibrational modes of the equatorial ligands and the symmetric or asymmetric modes of the actinyl ion. This was demonstrated by Jones showing that the M−L vibrational modes of the equatorial ligands can be ignored due

dx.doi.org/10.1021/ic401991n | Inorg. Chem. 2013, 52, 14138−14147

to their lack of significant coupling with the vibrational modes of the actinyl moiety, allowing for the AnO_2 unit to be treated as a linear triatomic molecule, thus simplifying the analysis of the spectra.[75] Additionally, our choice of cations aids in our analysis of the Raman and infrared spectra for the compounds presented here. The Rb^+ and Cs^+ cations were selected because their monatomic composition results in them being Raman and infrared silent, while the spectral contribution from the Me_4N^+ cation can be easily identified and accounted for through a comparison to the $[Me_4N]Cl$ salt (Figure S2 in the Supporting Information).

Triatomic molecules with a linear YXY arrangement ($D_{\infty h}$) such as the actinyl moiety (O═An═O) have three normal vibrational modes: a symmetric stretching mode (ν_1, Raman active), a bending mode (ν_2, infrared active), and an asymmetric stretching mode (ν_3, infrared active) (Supporting Information Figure S1).[76,77] In aqueous solution, it has been shown that these three modes of uranyl are typically observed between 860 and 880 cm^{-1} (ν_1), 199 and 210 cm^{-1} (ν_2), and 930 and 960 cm^{-1} (ν_3).[78] While significantly less is known about the plutonyl analogue, the symmetric[79] and asymmetric[78] stretching frequencies for $PuO_2(H_2O)_5^{2+}$ are located at 835 and 962 cm^{-1}, respectively. For the purposes of our discussion here, we will focus on the ν_1 and ν_3 stretching modes of the actinyl moiety since the ν_2 bending modes cannot be readily observed due to the wavelength limitations of our infrared spectrometer.

For uranyl complexes **U-Rb**, **U-Cs**, and **U-Me_4N**, the ν_1 symmetric stretch is the most prominent signal in the Raman spectrum and is observed as a sharp peak at 839, 832, and 831 cm^{-1}, respectively (Figure 3, Table 4). Similarly, the ν_3 asymmetric stretch appears in the infrared spectra as a strong signal located at 907 (**U-Rb**), 922 (**U-Cs**), and 909 cm^{-1} (**U-Me_4N**). These shifts for the symmetric and asymmetric stretches are similar to those previously observed for the $UO_2Cl_4^{2-}$ anion, which range from 831 to 842 cm^{-1} for ν_1 and 900 to 922 cm^{-1} for ν_3.[59−61,68,70−72,80] For compound **U-Cs**, in addition to the ν_1 signal at 832 cm^{-1}, a small peak is observed at 806 cm^{-1} corresponding to the $^{18}O═U═^{16}O$ symmetric stretching frequency, which agrees with the degree of red shifting expected for the monoisotopically substituted uranyl moiety.[81,82] Isotopic shifting of the ν_1 symmetric stretching frequency has been previously observed in di-isotopically substituted ^{18}O species uranyl hydroxide species, $U^{18}O_2(OH)_n^{2-n}$.[6]

Table 4. Symmetric (ν_1, cm^{-1}) and Asymmetric (ν_3, cm^{-1}) -yl Stretches for Complexes U-Rb, U-Cs, U-Me_4N, Pu-Rb, Pu-Cs, and Pu-Me_4N along with the Stretching Force Constant (k_1, mdyn/Å) and Interaction Force Constant (k_{12}, mdyn/Å) for the An═O Bond

compound	ν_1	ν_3	k_1	k_{12}
	Uranium			
UO_2^{2+} (aq)	860−880[78]	930−960[78]		
$Rb_2UO_2Cl_4{\cdot}2H_2O$ (**U-Rb**)	839	907	6.74	−0.10
$Cs_2UO_2Cl_4$ (**U-Cs**)	832	922	6.79	−0.27
$[Me_4N]_2UO_2Cl_4$ (**U-Me_4N**)	831	909	6.68	−0.18
	Plutonium			
$PuO_2(H_2O)_5^{2+}$	835[79]	962[78]		
$Rb_2PuO_2Cl_4$ (**Pu-Rb**)	810	932	6.69	−0.52
$Cs_2PuO_2Cl_4$ (**Pu-Cs**)	801	925	6.58	−0.53
$[Me_4N]_2PuO_2Cl_4$ (**Pu-Me_4N**)	793	909	6.39	−0.48

Upon traversing the actinide series from uranium to plutonium, the ν_1 symmetric stretching frequency undergoes a red shift of 30−40 cm^{-1} appearing at 810, 801, and 793 cm^{-1} for **Pu-Rb**, **Pu-Cs**, and **Pu-Me_4N**, respectively (Figure 3, Table 4). As with **U-Cs**, the Raman spectra for compounds **Pu-Rb** (785 cm^{-1}) and **Pu-Cs** (777 cm^{-1}) also contain small peaks corresponding to the monoisotopically substituted $^{18}O═Pu═^{16}O$ symmetric stretching frequency. Interestingly, unlike the ν_1 symmetric stretching frequency, a similar shift is not observed for the ν_3 asymmetric stretching frequency when traversing across the actinides. The infrared spectra of plutonyl compounds **Pu-Cs** (925 cm^{-1}) and **Pu-Me_4N** (909 cm^{-1}) exhibit almost no shift of the ν_3 signal in comparison to their isostructural uranyl analogues, while the asymmetric stretch for compound **Pu-Rb** (932 cm^{-1}) is blue-shifted 25 cm^{-1} from where it was observed for the hydrated uranyl species. The lack of shifting (or slight blue shift) for the O═An═O asymmetric stretching frequency (ν_3) when going from uranyl to plutonyl is very surprising considering the ν_1 symmetric stretch involves the same three atoms and undergoes a red shift of 30−40 cm^{-1}. This lack of synchronicity between the symmetric and asymmetric stretching frequencies is not readily understood, and future studies probing this phenomenon could elucidate significant information about the electronic structure of the actinyl moiety.

Unlike the easily identifiable ν_1 symmetric and ν_3 asymmetric stretches of the actinyl moiety, the metal−chloride based vibrations are more difficult to definitively assign due to their close proximity to one another. Our tentative assignments discussed in the Supporting Information are based on the relative positions of the signals observed in previously reported $AnO_2Cl_4^{2-}$ compounds.[39,59,61,66,70−72,80,83]

Actinyl Force Constants. The stretching force constant (k_1) and interaction force constant (k_{12}) for the An═O bond can be calculated from the symmetric (ν_1) and asymmetric stretches (ν_3) of the actinyl compound using a valence bond potential model.[76,81,84,85] The stretching force constant corresponds to the An═O bonds of the -yl moiety, while the interactive force constant describes the interaction between the two actinyl oxygen atoms. As stated previously it is possible to ignore the interaction between the uranyl moiety and its equatorial ligands in order to treat the O═An═O moiety as a linear triatomic molecule.[75] It should be noted that a harmonic model and the experimental values obtained for the ν_1 and ν_3 stretches are used for all of the calculations performed herein.

Utilizing our experimental values for the symmetric and asymmetric stretches of uranium compounds **U-Rb**, **U-Cs**, and **U-Me_4N**, we have calculated the stretching force constants to be 6.74, 6.79, and 6.68 mdyn/Å, respectively (Table 4). A slight decrease in k_1 is observed when traversing the actinides to the corresponding plutonium compounds **Pu-Rb** (6.69 mdyn/Å), **Pu-Cs** (6.58 mdyn/Å), and **Pu-Me_4N** (6.39 mdyn/Å). This decrease in the stretching force constant signifies a weakening of the An═O bond when transitioning from uranyl to plutonyl. While this is consistent with trends in the gas phase O═An═O bond dissociation energy when going from uranyl to plutonyl,[86] it is contradictory to what might be expected on the basis of the coinciding contraction of the An═O bond length, a relationship that will be discussed further in the following section.

A similar decrease is also observed when comparing the interaction force constant for the uranyl compound to those of the plutonyl compounds. For the uranium compounds, the

dx.doi.org/10.1021/ic401991n | Inorg. Chem. 2013, 52, 14138−14147

interaction force constants are −0.10, −0.27, and −0.18 mdyn/Å for compounds **U-Rb**, **U-Cs**, and **U-Me$_4$N**, respectively. These values become more negative upon navigating across the actinides to plutonium, where the analogous compounds have interaction force constants of −0.52 (**Pu-Rb**), −0.53 (**Pu-Cs**), and −0.48 (**Pu-Me$_4$N**).

DISCUSSION

Badger's Rule "Paradox". It has been almost 80 years since Badger published his formula derived from the transition metals (Badger's Rule) relating the equilibrium length (r_e) of a bond X−Y to its stretching force constant (k_1).[87,88] This relationship, expressed here, $k_1 = A(r_e - B)^{-3}$, relies on the use of a universal constant (A = 1.86 mdyn Å^2)[77,89] and a variable B that is based on the periodic rows within which elements X and Y reside.[90] While this formula has been shown to be significantly more accurate when calculating the bond length from the bond strength than vice versa,[89,90] it typically affirms the rule of thumb that a shorter bond has a larger stretching force constant. One of the many examples of this rule can be seen when comparing the experimentally determined bond lengths and stretching force constants for the metal−metal bond in V_2, Fe_2, and Cu_2.[89,91] Upon navigating the third row transition metals from vanadium to iron to copper, the length of the metal−metal bond increases from 1.77 to 2.02 to 2.22 Å concomitant with the stretching force constant decreasing from 4.34 to 1.48 to 1.30 (mdyn/Å), respectively. Jones explored the applicability of Badger's rule for relating the U=O bond length and force constants for uranyl complexes.[92] His analysis of a small sample of complexes showed that Badger's rule could be applied to uranyl, on the basis of the assumption that the normal modes of vibration for the uranyl moiety are decoupled from those of the equatorial ligands. While this is the case for the majority of uranyl compounds, it should be noted that a recent theoretical investigation showed significant mixing of the uranyl vibrations with the U−OH stretches in $[UO_2(OH)_4]^{2-}$ and $[UO_2(OH)_2(H_2O)_3]$, causing Badger's rule to be invalid for these compounds.[18]

Interestingly, the results presented herein suggest that the correlation between decreasing bond length and an increasing stretching force constant is not observed for isostructural compounds traversing the actinides. In this work, we present two sets of isostructural uranyl and plutonyl compounds, Cs compounds **U-Cs** and **Pu-Cs** and Me_4N compounds **U-Me$_4$N** and **Pu-Me$_4$N**, that can be used to examine the correlation between the An=O bond length and the stretching force constant. Although both compounds **U-Rb** and **Pu-Rb** have the same charge balancing cation (Rb), compound **U-Rb** crystallizes in the triclinic space group $P\bar{1}$ with two water molecules in the crystal lattice, while compound **Pu-Rb** crystallizes as the unsolvated species in the monoclinic space group $C2/m$. Due to the differences in both the crystallographic phase and solvation state of the compound, a direct comparison cannot be made because the magnitude of these influences upon the electronic structure of the actinyl moiety is unknown.

For compounds **U-Cs** and **Pu-Cs** and compounds **U-Me$_4$N** and **Pu-Me$_4$N**, there is a trend showing a slight decrease in the An=O bond length from uranium to plutonium. (While these values are statistically very similar, there is a decrease going from U to Pu based on the overall trend present when looking at experimental and theoretical data for a broader range of An—O and An=O interactions found in compounds such as $AnO_2(H_2O)_5^{2+}$ (An = U, Np, Pu),[93] $AnO_2(NO_3)_2(H_2O)_2$ (An = U, Pu),[94] $AnO_2(SO_4)(H_2O)_3$ (An = U, Pu),[94] $K_4AnO_2(CO_3)_3$ (An = U, Np),[95,96] AnO_2 (An = Th, Pa, U, Np, Pu, Am),[97] $An(^{Ar}acnac)_4$ (An = Th, U, Pu),[98] $[An(\alpha_2\text{-}P_2W_{17}O_{61})_2]^{16-}$ (An = Th, U, Np, Pu, Am),[99] and $\{C(NH_2)_3\}_4[An(C_2O_4)_4]\cdot 2H_2O$ (An = Th, U, Pu).[100]) Interestingly, the stretching force constant also decreases 0.21 mdyn/Å between **U-Cs** and **Pu-Cs**, and 0.29 mdyn/Å between **U-Me$_4$N** and **Pu-Me$_4$N** when transitioning from uranyl to plutonyl (Table 4). These results are consistent with an earlier discussion by Tait et al. where they observed a decrease in both bond length and strength when navigating across the actinides.[101]

The phenomenon of a concomitant decrease in both bond length and stretching force constant across the actinides is not completely understood, but one explanation is that it arises from the actinide contraction.[101] Similar to the lanthanide contraction, the actinide contraction is the decrease in the atomic radius and contraction of the bonding orbitals when traversing left to right across the actinides that arises from inefficient shielding of the increasing nuclear charge by the valence electrons. In isostructural compounds across the actinides, the decrease in the atomic radius manifests itself as a shortening in the metal−ligand bond length, while the simultaneous contraction of the actinide 5f and 6d orbitals weakens the bond due to the decrease in orbital overlap with the ligand.[101] This explanation fits well with the experimental results for the Cs and Me_4N compounds presented here, where the shortening of the An=O bond length (Cs, 0.03 Å; Me_4N, 0.02 Å) (Table 2) going from uranium to plutonium correlates well with the 0.2 Å contraction in ionic radius from U(VI) (0.73 Å) to Pu(VI) (0.71 Å).[43]

In addition to the actinide contraction, another contributing factor to the weakening of the An=O bond when going from U to Pu could be the presence of the two f-electrons in Pu(VI). In plutonyl, these 2 f-electrons are located in the δ_u nonbonding orbital.[102] For uranyl, Denning has shown that the δ_u nonbonding orbital mixes with the π_u antibonding orbital due to spin−orbit coupling resulting in a configuration interaction between the $\sigma_u\pi_u$ and $\sigma_u\delta_u$.[1] Therefore, the presence of the two 5f electrons in Pu(VI) may indicate greater antibonding character in the plutonyl versus uranyl bond, resulting in a reduced force constant.

Inverse Trans Influence. A negative interaction force constant for linear triatomic centrosymmetric molecules, such as the actinyl moiety in the compounds presented here, corresponds to a reduction of the force constant for the symmetric stretching mode. The root of this can be seen by examining the general potential function for a symmetric linear triatomic molecule shown in eq 1.[76,81,84] In the symmetric stretching mode, both Δr_1 and Δr_2 possess the same sign, meaning a negative interactive force constant (k_{12}) lowers the energy of the symmetric stretch. Reduction of the force constant for the symmetric stretch has been described as a dynamic manifestation of the actinide inverse trans influence.[4]

$$2V = k_1(\Delta r_1^2 + \Delta r_2^2) + 2k_{12}(\Delta r_1 \Delta r_2) + k_\delta \delta^2 \quad (1)$$

This can be seen experimentally by comparing the relative energies of the symmetric and asymmetric stretching frequencies for the compounds presented here. The symmetric stretching mode of the actinyl moiety appears at a lower energy than the asymmetric stretching mode (Figure 3, Table 4). This can be thought of as the two An=O bonds working in tandem due to the inverse trans influence, which results in a negative

interaction force constant for all of the actinyl compounds. In contrast to the inverse trans influence experienced by the actinyls, isostructural transition metal dioxo compounds typically abide by the normal trans influence, where the trans metal−oxo bonds work in competition with each other resulting in a positive interaction force constant and a decrease of the force constant for the asymmetric stretching mode. In compounds such as $K_2[OsO_2Cl_4]$ (ν_1, 904; ν_3, 837 cm^{-1}; k_{12}, 1.03 mdyn/Å) and $K_3[ReO_2(CN)_4]$ (ν_1, 871; ν_3, 768 cm^{-1}; k_{12}, 1.28 mdyn/Å),[103,104] the normal trans influence is manifested through a positive interaction force constant and the O═TM═O asymmetric stretching mode appearing at a lower energy than the symmetric stretching mode.

Cation Influences. The compounds presented here also afford us the opportunity to indirectly probe the influence of the cation upon the electronic structure of the actinyl moiety. Plutonyl compounds **Pu-Rb** and **Pu-Cs** are isostructural and isoelectronic, varying only by the identity of the cation. The difference between the two stretching force constants for compounds **Pu-Rb** and **Pu-Cs** is only 0.11 mdyn/Å, in comparison to the 0.21 mdyn/Å difference that is present between isostructural compounds **U-Cs** and **Pu-Cs** where the identity of the actinide metal changes (Table 4). While the conclusion is not surprising, this comparison illustrates that, in this case, the identity of the metal center is significantly more influential upon the electronic structure of the actinyl moiety than the identity of the countercation.

CONCLUSION

In this work, we report the crystallographic and spectroscopic characterization of three uranyl and three plutonyl compounds. Using the experimental values for the symmetric and asymmetric stretches of the actinyl moieties, we calculated the stretching force constant and interaction force constant for each of the compounds. The calculated stretching force constants demonstrate a weakening of the An═O bond when traversing the actinides from uranium to plutonium. This is somewhat counterintuitive since replacing uranium with plutonium results in a slight contraction of the An═O bond length in the solid state molecular structure. Additionally, the interaction force constants for both the uranyl and plutonyl compounds were found to be negative, which corresponds to a reduction of the force constant for the symmetric stretching mode and is a manifestation of the inverse trans influence that occurs in actinide compounds.

Further studies will continue to address the differences in the electronic structure of the actinyl ion as well as aim to quantify the influence from lattice solvent and the crystallographic phase upon the electronic structure of the actinyl moiety. We also plan to continue to probe the behavior of the actinyl symmetric and asymmetric stretching frequencies that occurs while traversing the actinides from uranium to plutonium (ν_1 undergoes a red shift but ν_3 stays the same or displays a blue shift) because we believe it contains valuable information about the electronic structure of the actinyl moiety. Additionally, we believe future investigations involving quantum mechanical calculations as well as optical and luminescence spectroscopy could complement these studies nicely.

ASSOCIATED CONTENT

Supporting Information

Crystallographic information in CIF format, compound peak information and assignments, additional vibrational analysis, molecular site analysis, detailed calculations for isotopic shifting and force constants, solid state molecular structures with 50% probability ellipsoids, IR (400−5000 cm^{-1}) spectra, and Raman spectra (100−4000 cm^{-1}) for the reported complexes. This material is available free of charge via the Internet at http://pubs.acs.org.

AUTHOR INFORMATION

Corresponding Author

*E-mail: rewilson@anl.gov.

Notes

The authors declare no competing financial interest.

ACKNOWLEDGMENTS

This work was performed at Argonne National Laboratory, operated for the United States Department of Energy, Office of Science, Office of Basic Energy Sciences, by UChicagoArgonne LLC under Contract DE-AC02-06CH11357.

REFERENCES

(1) Denning, R. G. *J. Phys. Chem. A* **2007**, *111* (20), 4125−4143.
(2) Darwent, B. deB. *Nat. Stand. Ref. Data Ser.* **1970**, *31*, 1−48.
(3) Butcher, R. J.; Penfold, B. R.; Sinn, E. *J. Chem. Soc., Dalton Trans.* **1979**, *0* (4), 668−675.
(4) Denning, R. G. Electronic Structure and Bonding in Actinyl Ions. In *Structure and Bonding: Complexes, Clusters and Crystal Chemistry*; Clarke, M. J., Goodenough, J. B., Ibers, J. A., Jørgensen, C. K., Mingos, D. M. P., Neilands, J. B., Palmer, G. A., Reinen, D., Sadler, P. J., Weiss, R., Williams, J. P., Eds.; Springer-Verlag: New York, 1992; Vol. *79*, pp 215−276.
(5) Cotton, S. A. *Lanthanide and Actinide Chemistry*; John Wiley and Sons, Ltd.: Chichester, U.K., 2006.
(6) Clark, D. L.; Conradson, S. D.; Donohoe, R. J.; Keogh, D. W.; Morris, D. E.; Palmer, P. D.; Rogers, R. D.; Tait, C. D. *Inorg. Chem.* **1999**, *38* (7), 1456−1466.
(7) Gordon, G.; Taube, H. *J. Inorg. Nucl. Chem.* **1961**, *19* (1−2), 189−191.
(8) Gaziev, S. A.; Gorshkov, N. G.; Mashirov, L. G.; Suglobov, D. N. *Radiokhimiya* **1986**, *28* (6), 770−772.
(9) Gaziev, S. A.; Gorshkov, N. G.; Mashirov, L. G.; Suglobov, D. N. *Radiokhimiya* **1986**, *28* (6), 764−770.
(10) Gaziev, S. A.; Gorshkov, N. G.; Mashirov, L. G.; Suglobov, D. N. *Radiokhimiya* **1986**, *28* (6), 755−763.
(11) Toth, L. M.; Begun, G. M. *J. Phys. Chem.* **1981**, *85* (5), 547−549.
(12) Fillaux, C.; Guillaumont, D.; Berthet, J.-C.; Copping, R.; Shuh, D. K.; Tyliszczak, T.; Auwer, C. D. *Phys. Chem. Chem. Phys.* **2010**, *12* (42), 14253−14262.
(13) Fortier, S.; Hayton, T. W. *Coord. Chem. Rev.* **2010**, *254* (3−4), 197−214.
(14) Tsushima, S. *Dalton Trans.* **2011**, *40* (25), 6732−6737.
(15) Allen, P. G.; Bucher, J. J.; Clark, D. L.; Edelstein, N. M.; Ekberg, S. A.; Gohdes, J. W.; Hudson, E. A.; Kaltsoyannis, N.; Lukens, W. W.; Neu, M. P.; Palmer, P. D.; Reich, T.; Shuh, D. K.; Tait, C. D.; Zwick, B. D. *Inorg. Chem.* **1995**, *34* (19), 4797−4807.
(16) Ingram, K. I. M.; Haller, L. J. L.; Kaltsoyannis, N. *Dalton Trans.* **2006**, *0* (20), 2403−2414.
(17) McGlynn, S. P.; Smith, J. K.; Neely, W. C. *J. Chem. Phys.* **1961**, *35* (1), 105−116.
(18) Vallet, V.; Wahlgren, U.; Grenthe, I. *J. Phys. Chem. A* **2012**, *116* (50), 12373−12380.
(19) Groenewold, G. S.; Gianotto, A. K.; Cossel, K. C.; Van Stipdonk, M. J.; Moore, D. T.; Polfer, N.; Oomens, J.; de Jong, W. A.; Visscher, L. *J. Am. Chem. Soc.* **2006**, *128* (14), 4802−4813.
(20) Groenewold, G. S.; Gianotto, A. K.; McIlwain, M. E.; Van Stipdonk, M. J.; Kullman, M.; Moore, D. T.; Polfer, N.; Oomens, J.;

Infante, I.; Visscher, L.; Siboulet, B.; de Jong, W. A. *J. Phys. Chem. A* **2008**, *112* (3), 508−521.
(21) Nguyen Trung, C.; Begun, G. M.; Palmer, D. A. *Inorg. Chem.* **1992**, *31* (25), 5280−5287.
(22) Sarsfield, M. J.; Helliwell, M.; Raftery, J. *Inorg. Chem.* **2004**, *43* (10), 3170−3179.
(23) Burns, C. J.; Clark, D. L.; Donohoe, R. J.; Duval, P. B.; Scott, B. L.; Tait, C. D. *Inorg. Chem.* **2000**, *39* (24), 5464−5468.
(24) Sarsfield, M. J.; Helliwell, M. *J. Am. Chem. Soc.* **2004**, *126* (4), 1036−1037.
(25) Arnold, P. L.; Hollis, E.; Nichol, G. S.; Love, J. B.; Griveau, J.-C.; Caciuffo, R.; Magnani, N.; Maron, L.; Castro, L.; Yahia, A.; Odoh, S. O.; Schreckenbach, G. *J. Am. Chem. Soc.* **2013**, *135* (10), 3841−3854.
(26) Arnold, P. L.; Pécharman, A.-F.; Love, J. B. *Angew. Chem., Int. Ed.* **2011**, *50* (40), 9456−9458.
(27) Brown, J. L.; Mokhtarzadeh, C. C.; Lever, J. M.; Wu, G.; Hayton, T. W. *Inorg. Chem.* **2011**, *50* (11), 5105−5112.
(28) Schnaars, D. D.; Wu, G.; Hayton, T. W. *J. Am. Chem. Soc.* **2009**, *131* (48), 17532−17533.
(29) Schnaars, D. D.; Wu, G.; Hayton, T. W. *Inorg. Chem.* **2011**, *50* (19), 9642−9649.
(30) Schnaars, D. D.; Wu, G.; Hayton, T. W. *Inorg. Chem.* **2011**, *50* (11), 4695−4697.
(31) *Bruker APEX2 Software Suite, APEX2 v2011.4-1*; Bruker AXS: Madison, WI, 2011.
(32) Steiner, T. *Acta Crystallogr.* **1998**, *B54* (4), 456−463.
(33) Fujita, K.; MacFarlane, D. R.; Noguchi, K.; Ohno, H. *Acta Crystallogr.* **2009**, *E65* (4), o797.
(34) Spek, A. L. *J. Appl. Crystallogr.* **2003**, *36*, 7−13.
(35) Anson, C. E.; AlJowder, O.; Jayasooriya, U. A.; Powell, A. K. *Acta Crystallogr.* **1996**, *C52*, 279−281.
(36) Hall, D.; Rae, A. D.; Waters, T. N. *Acta Crystallogr.* **1966**, *20*, 160−162.
(37) Watkin, D. J.; Denning, R. G.; Prout, K. *Acta Crystallogr.* **1991**, *C47*, 2517−2519.
(38) Di Sipio, L.; Tondello, E.; Pelizzi, G.; Ingletto, G.; Montenero, A. *Cryst. Struct. Commun.* **1974**, *3*, 297−300.
(39) Wilkerson, M. P.; Scott, B. L. *Acta Crystallogr.* **2008**, *E64*, i5.
(40) Bois, C.; Dao, N. Q.; Rodier, N. *Acta Crystallogr.* **1976**, *B32*, 1541−1544.
(41) Rogers, R. D.; Kurihara, L. K.; Benning, M. M. *Inorg. Chem.* **1987**, *26* (26), 4346−4352.
(42) Bombieri, G.; Forsellini, E.; Graziani, R. *Acta Crystallogr.* **1978**, *B34* (8), 2622−2624.
(43) Shannon, R. D. *Acta Crystallogr.* **1976**, *A32* (Sep1), 751−767.
(44) Berthon, C.; Boubals, N.; Charushnikova, I. A.; Collison, D.; Cornet, S. M.; Auwer, C.; Gaunt, A. J.; Kaltsoyannis, N.; May, I.; Petit, S.; Redmond, M. P.; Reilly, S. D.; Scott, B. L. *Inorg. Chem.* **2010**, *49* (20), 9554−9562.
(45) Gaunt, A. J.; Reilly, S. D.; Hayton, T. W.; Scott, B. L.; Neu, M. P. *Chem. Commun.* **2007**, *16*, 1659−1661.
(46) Taylor, J. R. *An Introduction to Error Analysis: The Study of Uncertainties in Physical Measurements*; University Science Books: Sausalito, CA, 1997.
(47) Bondi, A. *J. Phys. Chem.* **1964**, *68* (3), 441−451.
(48) Trujillo, M.; Husted, R.; Boorman, M.; Hobart, D. E.; Smith, J. *Periodic Table of Elements: LANL*. http://periodic.lanl.gov/index.shtml (accessed January 22, 2013).
(49) Cotton, F. A.; Wilkinson, G.; Murillo, C. A.; Bochmann, M., *Advanced Inorganic Chemistry*, 6th ed.; Wiley: New York, 1999.
(50) Barnhart, D. M.; Burns, C. J.; Sauer, N. N.; Watkin, J. G. *Inorg. Chem.* **1995**, *34* (16), 4079−4084.
(51) Chen, F.; Wang, C.; Shi, W.; Zhang, M.; Liu, C.; Zhao, Y.; Chai, Z. *CrystEngComm* **2013**, *15* (39), 8041−8048.
(52) Danis, J. A.; Lin, M. R.; Scott, B. L.; Eichhorn, B. W.; Runde, W. H. *Inorg. Chem.* **2001**, *40* (14), 3389−3394.
(53) Thuery, P.; Masci, B. *Dalton Trans.* **2003**, *12*, 2411−2417.
(54) Choppin, G. R. *Radiochim. Acta* **1983**, *32*, 43−53.
(55) Choppin, G. R.; Rao, L. F. *Radiochim. Acta* **1984**, *37*, 143−146.
(56) Hemmingsen, L.; Amara, P.; Ansoborlo, E.; Field, M. J. *J. Phys. Chem. A* **2000**, *104* (17), 4095−4101.
(57) Brammer, L.; Bruton, E. A.; Sherwood, P. *Cryst. Growth Des.* **2001**, *1* (4), 277−290.
(58) Franczyk, T. S.; Czerwinski, K. R.; Raymond, K. N. *J. Am. Chem. Soc.* **1992**, *114* (21), 8138−8146.
(59) Flint, C. D.; Tanner, P. A. *Mol. Phys.* **1981**, *44* (2), 411−425.
(60) Ohwada, K. *J. Inorg. Nucl. Chem.* **1978**, *40* (7), 1369−1374.
(61) Ohwada, K. *Appl. Spectrosc.* **1980**, *34* (3), 327−331.
(62) Vdovenko, V. M.; Ladygin, I. N.; Suglobov, D. N. *Russ. J. Inorg. Chem.* **1968**, *13* (1), 154−156.
(63) Belyaev, Y. I.; Vdovenko, V. M.; Ladygin, I. N.; Suglobov, D. N. *Russ. J. Inorg. Chem.* **1967**, *12* (11), 1705−1706.
(64) Bullock, J. I. *J. Chem. Soc. A* **1969**, 781−784.
(65) Bullock, J. I.; Parrett, F. W. *Can. J. Chem.* **1970**, *48* (19), 3095−3097.
(66) Denning, R. G.; Snellgrove, T. R.; Woodwark, D. R. *Mol. Phys.* **1976**, *32* (2), 419−442.
(67) Dieke, G. H.; Duncan, A. B. F. *Spectroscopic Properties of Uranium Compounds*; McGraw-Hill Book Company, Inc.: New York, 1949.
(68) Flint, C. D.; Tanner, P. A. *J. Chem. Soc., Faraday Trans. 2* **1978**, *74*, 2210−2217.
(69) Matsika, S.; Pitzer, R. M. *J. Phys. Chem. A* **2000**, *105* (3), 637−645.
(70) Newbery, J. E. *Spectrochim. Acta. A* **1969**, *25* (10), 1699−1702.
(71) Ohwada, K. *Spectrochim. Acta. A* **1975**, *31* (7), 973−977.
(72) Flint, C. D.; Tanner, P. A. *J. Chem. Soc., Faraday Trans. 2* **1981**, *77* (10), 1865−1878.
(73) Volod'ko, L. V.; Komyak, A. I.; Posledovich, M. R. *J. Appl. Spectrosc.* **1968**, *8* (4), 390−392.
(74) Wilkerson, M. P.; Berg, J. M. *J. Phys. Chem. A* **2008**, *112* (12), 2515−2518.
(75) Jones, L. H. *Spectrochim. Acta* **1958**, *10* (4), 395−403.
(76) Herzberg, G. *Infrared and Raman Spectra of Polyatomic Molecules*; D. Van Nostrand Company, Inc.: New York, 1946.
(77) Nakamoto, K. *Infrared and Raman Spectra of Inorganic and Coordination Compounds Part A: Theory and Applications in Inorganic Chemistry*, 5th ed.; John Wiley & Sons, Inc.: New York, 1997.
(78) Jones, L. H.; Penneman, R. A. *J. Chem. Phys.* **1953**, *21* (3), 542−544.
(79) Basile, L. J.; Sullivan, J. C.; Ferraro, J. R.; LaBonville, P. *Appl. Spectrosc.* **1974**, *28* (2), 142−145.
(80) Gál, M.; Goggin, P. L.; Mink, J. *Spectrochim. Acta. A* **1992**, *48* (1), 121−132.
(81) See Supporting Information.
(82) Gillet, P.; McMillan, P.; Schott, J.; Badro, J.; Grzechnik, A. *Geochim. Cosmochim. Acta* **1996**, *60* (18), 3471−3485.
(83) Denning, R. G.; Norris, J. O. W.; Brown, D. *Mol. Phys.* **1982**, *46* (2), 287−323.
(84) Bader, R. F. W. *Mol. Phys.* **1960**, *3* (2), 137−151.
(85) Wilkins, R. W. T. *Z. Kristallogr.* **1971**, *134* (3−4), 285−290.
(86) Gibson, J. K.; Haire, R. G.; Santos, M.; Marçalo, J.; Pires de Matos, A. *J. Phys. Chem. A* **2005**, *109* (12), 2768−2781.
(87) Badger, R. M. *J. Chem. Phys.* **1934**, *2* (3), 128−131.
(88) Badger, R. M. *J. Chem. Phys.* **1935**, *3* (11), 710−714.
(89) Weisshaar, J. C. *J. Chem. Phys.* **1989**, *90* (3), 1429−1433.
(90) Cioslowski, J.; Liu, G.; Mosquera Castro, R. A. *Chem. Phys. Lett.* **2000**, *331* (5−6), 497−501.
(91) Moskovits, M.; DiLella, D. P.; Limm, W. *J. Chem. Phys.* **1984**, *80* (2), 626−633.
(92) Jones, L. H. *Spectrochim. Acta* **1959**, *15* (0), 409−411.
(93) Hay, P. J.; Martin, R. L.; Schreckenbach, G. *J. Phys. Chem. A* **2000**, *104* (26), 6259−6270.
(94) Craw, J. S.; Vincent, M. A.; Hillier, I. H.; Wallwork, A. L. *J. Phys. Chem.* **1995**, *99* (25), 10181−10185.
(95) Anderson, A.; Chieh, C.; Irish, D. E.; Tong, J. P. K. *Can. J. Chem.* **1980**, *58* (16), 1651−1658.

(96) Gorbeko-Germanov, D. S.; Klimov, V. C. *Russ. J. Inorg. Chem.* **1966**, *11* (3), 280−282.
(97) Seaborg, G. T. Paper 21.1: Electronic Structure of the Heaviest Elements. In *The Transuranium Elements: Research Papers*; McGraw-Hill Book Co. Inc.: New York, 1949; Vol. *2*.
(98) Schnaars, D. D.; Gaunt, A. J.; Hayton, T. W.; Jones, M. B.; Kirker, I.; Katsoyannis, N.; May, I.; Reilly, S. D.; Scott, B. L.; Wu, G. *Inorg. Chem.* **2012**, *51* (15), 8557−8566.
(99) Sokolova, M. N.; Fedosseev, A. M.; Andreev, G. B.; Budantseva, N. A.; Yusov, A. B.; Moisy, P. *Inorg. Chem.* **2009**, *48* (19), 9185−9190.
(100) Andreev, G.; Budantseva, N.; Fedoseev, A.; Moisy, P. *Inorg. Chem.* **2011**, *50* (22), 11481−11486.
(101) Tait, C. D.; Donohoe, R. J.; Clark, D. L.; Conradson, S. D.; Ekberg, S. A.; Keogh, D. W.; Neu, M. P.; Reilly, S. D.; Runde, W. H.; Scott, B. L. *Actinide Research Quarterly*; Report LA-LP-04−60; Los Alamos National Laboratory: Los Alamos, NM, 2004; Vol. *1*, pp 20−22.
(102) Morss, L. R.; Edelstein, N. M.; Fuger, J.; Katz, J. J. *The Chemistry of the Actinide and Transactinide Elements*, 3rd ed.; Springer: Dordrecht, 2006.
(103) Griffith, W. P. *J. Chem. Soc.* **1964**, 245−249.
(104) Griffith, W. P. *J. Chem. Soc. A* **1969**, 211−218.